

Fe I and Fe II ABUNDANCES OF SOLAR-TYPE DWARFS IN THE PLEIADES OPEN CLUSTER¹

Simon C. Schuler^{2,3}

National Optical Astronomy Observatory/Cerro Tololo Inter-American Observatory

Casilla 603, La Serena, Chile

`sschuler@noao.edu`

Adele L. Plunkett^{4,5}

Department of Physics, Middlebury College

McCardell Bicentennial Hall, Middlebury, VT 05753

`aplunket@middlebury.edu`

Jeremy R. King

Department of Physics and Astronomy, Clemson University

118 Kinard Laboratory, Clemson, SC 29634

`jking2@ces.clemson.edu`

and

Marc H. Pinsonneault

Department of Astronomy, Ohio State University

140 West 18th Avenue, Columbus, OH 43210

`pinsono@astronomy.ohio-state.edu`

¹Based on observations obtained with the High Resolution Spectrograph on the Hobby - Eberly Telescope, which is operated by McDonald Observatory on behalf of the University of Texas at Austin, the Pennsylvania State University, Stanford University, the Ludwig-Maximilians-Universitaet, Munich, and the George-August-Universitaet, Goettingen. Public Access time on the Hobby - Eberly Telescope administered through the National Optical Astronomy Observatory was made possible through an agreement with the National Science Foundation.

²Current address: NOAO, 950 North Cherry Avenue, Tucson, AZ 85719

³Leo Goldberg Fellow

⁴Visiting Astronomer, NOAO/CTIO, Casilla 603, La Serena, Chile

⁵Current address: Department of Astronomy, Yale University, New Haven, CT 06520-8101

ABSTRACT

We have derived Fe abundances of 16 solar-type Pleiades dwarfs by means of an equivalent width analysis of Fe I and Fe II lines in high-resolution spectra obtained with the Hobby - Eberly Telescope and High Resolution Spectrograph. Abundances derived from Fe II lines are larger than those derived from Fe I lines (herein referred to as over-ionization) for stars with $T_{\text{eff}} < 5400$ K, and the discrepancy ($\Delta\text{Fe} = [\text{Fe II}/\text{H}] - [\text{Fe I}/\text{H}]$) increases dramatically with decreasing T_{eff} , reaching over 0.8 dex for the coolest stars of our sample. The Pleiades joins the open clusters M 34, the Hyades, IC 2602, and IC 2391, and the Ursa Major moving group, demonstrating ostensible over-ionization trends. The Pleiades ΔFe abundances are correlated with Ca II infrared triplet and H α chromospheric emission indicators and relative differences therein. Oxygen abundances of our Pleiades sample derived from the high-excitation O I triplet have been previously shown to increase with decreasing T_{eff} , and a comparison with the ΔFe abundances suggests that the over-excitation (larger abundances derived from high excitation lines relative to low excitation lines) and over-ionization effects that have been observed in cool open cluster and disk field main sequence (MS) dwarfs share a common origin. Curiously, a correlation between the Pleiades O I abundances and chromospheric emission indicators does not exist. Star-to-star Fe I abundances have low internal scatter (< 0.11 dex), but the abundances of stars with $T_{\text{eff}} < 5400$ K are systematically higher compared to the warmer stars. The cool star [Fe I/H] abundances cannot be connected directly to over-excitation effects, but similarities with the ΔFe and O I triplet trends suggest the abundances are dubious. Using the [Fe I/H] abundances of five stars with $T_{\text{eff}} > 5400$ K, we derive a mean Pleiades cluster metallicity of $[\text{Fe}/\text{H}] = +0.01 \pm 0.02$.

Subject headings: open clusters and associations:individual (Pleiades) — stars:abundances — stars:atmospheres — stars:late-type

1. INTRODUCTION

Studies of Galactic chemical evolution are dependent on accurately derived abundances of stars spanning all ages, populations, kinematics, masses, and metallicities. Stars with masses $M \leq 1M_{\odot}$ are especially important given their dominance of the initial mass function (IMF; e.g., Kroupa 2002). Abundance studies utilizing high-resolution spectroscopy and local thermodynamic equilibrium (LTE) analyses of near-solar metallicity G and K dwarfs

in open clusters and in the disk field, however, have revealed that the observed abundances of at least some elements derived for these cool main sequence (MS) dwarfs may be spurious. In particular, studies have found evidence of over-ionization and over-excitation⁶, i.e., larger abundances are derived from lines of singly ionized species compared to neutral species and from high-excitation lines of neutral species compared to low-excitation lines, respectively. The first indication that some abundances derived for cool MS stars are problematic may have come from Oinas (1974), who found the over-ionization of Sc, Ti, Cr, and Fe for a sample of 10 K dwarfs ($4800 \leq T_{\text{eff}} \leq 5600$ K) in the solar neighborhood. After a careful analysis of the procedures and stellar parameters used in the abundance derivations, the author was unable to account for the overabundances of the ionized species. Feltzing & Gustafsson (1998) found similar over-ionization results for Sc, V, Cr, Fe, and Y in five field K dwarfs ($4510 \leq T_{\text{eff}} \leq 4833$ K). The authors could not exclude an inaccurate temperature scale that is several hundred K too low as a possible source of the anomalous abundances, but in the end, they suggest that non-LTE (NLTE) effects are the more likely cause.

Open clusters have been important to the identification and continued study of the over-excitation/ionization effects, because the presumed internal chemical homogeneity of the clusters provides a baseline with which anomalous abundances can be compared. King et al. (2000a) derived O abundances from the high-excitation ($\chi = 9.15$ eV) near-IR O I triplet of a K dwarf in each of the the Pleiades and NGC 2264 open clusters, and in both cases, the abundances were highly enhanced: $[\text{O}/\text{H}] = +0.85$ and $+0.43$, respectively. Such high O abundances are not expected for clusters with nominal metallicities of $[\text{Fe}/\text{H}] = 0.00$ (Boesgaard et al. 1988) and -0.15 (King et al. 2000a), respectively. Following King et al. (2000a), Schuler et al. (2003) derived the abundances of MS dwarfs in the M 34 cluster; over-ionization of Fe and over-excitation of Si (the abundances of which were derived from lines with excitation potentials in the range $5.61 \leq \chi \leq 6.19$ eV) are seen in the coolest stars of the sample. Oxygen abundances of the cool M 34 dwarfs, as well as cool Pleiades dwarfs, derived from the high-excitation O I triplet are also highly enhanced (Schuler et al. 2004), confirming the earlier results of King et al. (2000a).

Subsequent to these early open cluster studies, the over-ionization of Fe has been confirmed in the Hyades (Yong et al. 2004; Schuler et al. 2006a) and Ursa Major (UMa) moving group (King & Schuler 2005), and of Ti in the young pre-MS clusters IC 2602 and IC 2391

⁶In this paper, we use over-ionization and over-excitation to refer to the observed enhanced abundances derived from spectral lines of singly ionized species or from high excitation lines, as opposed to other common usages referring specifically to the non-LTE (NLTE) effects of over-ionization (the mean intensity, J_ν , is larger than the Planck function, B_ν , in lower atomic energy levels), resonance scattering, and photon pumping (e.g., Feltzing & Gustafsson 1998; Asplund 2005).

(D’Orazi & Randich 2009). Overabundances of O derived from the O I triplet have been reported for the UMa moving group (King & Schuler 2005), the Hyades (Schuler et al. 2006b), and IC 4665 (Shen et al. 2007). Over-excitation effects have been reported for other elements, as well, including S in the Pleiades (Schuler et al. 2004), Si, Ti, Ni, and Cr in IC 4665 (Shen et al. 2005), Ni in the Hyades (Schuler et al. 2006a), and Ca, Ti, and Na in IC 2602 and IC 2391 (D’Orazi & Randich 2009). Recent abundance analyses of cool field stars have also identified over-excitation/ionization effects (Allende Prieto et al. 2004; Ramírez et al. 2007; Chen et al. 2008), confirming the findings of earlier work.

The over-excitation/ionization abundance anomalies are not thought to represent real photospheric overabundances; rather, we believe that they are a signal that our knowledge of cool dwarf atmospheres and/or spectral line formation therein is incomplete. As of yet, the source or cause of the effects has not been identified. Systematically erroneous stellar parameters, e.g., an inaccurate T_{eff} scale, could lead to the observed abundance trends, but in general, unrealistically large parameter errors would have to be present (e.g., King & Schuler 2005; Schuler et al. 2006b). Furthermore, parameter changes made in response to the overabundances of one element often increase those of another (e.g., Schuler et al. 2003). NLTE effects have been suggested as the cause (e.g., Feltzing & Gustafsson 1998), but in general, the over-excitation/ionization effects seen in cool dwarfs are in stark contrast to extant NLTE calculations. For instance, LTE analyses of the high-excitation O I triplet in the spectra of MS dwarfs are predicted to result in increasingly discrepant abundances with increasing T_{eff} for stars with $T_{\text{eff}} > 6000$ K, requiring negative NLTE corrections up to 0.4 – 0.5 dex at 6500 K for solar metallicity dwarfs (Takeda 2003; Fabbian et al. 2009). Below 6000 K, the NLTE corrections are predicted to be < 0.1 dex and essentially zero below 5500 K (Takeda 2003). Chromospheric emission and photospheric activity (spots, plages, and faculae) have also been suggested sources for the abundance anomalies (e.g., Schuler et al. 2006b). These inhomogeneities could produce apparent over-excitation/ionization effects within a strict LTE framework.

Continuing our efforts to delineate and understand the observed over-excitation/ionization effects in cool MS dwarfs, we have derived Fe I and Fe II abundances of 16 Pleiades dwarfs, 15 of which have had O abundances derived from the high-excitation O I triplet (Schuler et al. 2004). The O I abundances evince a steep increase, reaching $[\text{O}/\text{H}] \approx 1.0$ dex near 5000 K, and star-to-star dispersion below 5500 K. We use the newly derived Pleiades Fe abundances to investigate if the over-excitation and over-ionization effects observed in cool MS dwarfs are related and indeed manifestations of the same phenomenon. Future observational studies that could place stringent constraints on these effects and bring us closer to discovering the source of the anomalous abundances are also discussed.

2. OBSERVATIONS AND ANALYSIS

Echelle spectra of 17 Pleiades MS dwarfs were obtained with the 9.2-m Hobby - Eberly Telescope (HET) and High Resolution Spectrograph (HRS) at the McDonald Observatory in queue-mode on 22 separate nights between 2002 August 23 UT and 2003 February 17 UT. These spectra have been used previously by Schuler et al. (2004) and King et al. (2010) who analyzed the $\lambda 7775$ O I high-excitation triplet and the $\lambda 6707$ Li I line, respectively, in these Pleiades dwarfs; please consult these papers for detailed descriptions of the observations and spectra. Briefly, the HET/HRS detector is a 4096 x 4100 side-by-side CCD mosaic of two 2048 x 4100 CCDs with 15 μm pixels. The spectra are characterized by a high resolution of $R \equiv \lambda/\Delta\lambda = 60,000$, and they have typical signal-to-noise (S/N) ratios of 80 – 100. The spectra cover the wavelengths 5095 to 8860 Å. Data reduction followed the typical practice of using standard IRAF routines to remove the bias pattern, subtract scattered light, flat-field, and wavelength-calibrate the spectra. The stars in our sample are listed in Table 1.

Nineteen Fe I and seven Fe II lines spanning 5793 to 7462 Å have been analyzed in the spectra of 16 of the seventeen Pleiads in our sample; note, however, that not all of the lines were measurable in all of the stars. Equivalent widths (EWs) were determined by fitting each line with a Gaussian profile using the one-dimensional spectrum analysis software package SPECTRE (Fitzpatrick & Sneden 1987). The EW measurements, along with the wavelength, excitation potential (χ), and transition probabilities ($\log gf$) of each line, are given in Tables 2 – 4. Atomic data of the lines were obtained by email query to the Vienna Atomic Line Database (VALD) (Piskunov et al. 1995; Kupka et al. 1999; Ryabchikova et al. 1999).

One star included in our Li study (King et al. 2010) but not considered here is H II 152. This star was observed on two nights separated by approximately ten months. As discussed by King et al., target misidentification on one night is a concern. On the night where it is not a concern, the spectra were obtained with a grating setting distinct from the setting used for the other stars in our sample, giving a spectral coverage of 6100 to 9800 Å. Many of the Fe I and Fe II lines in our linelist fall outside of the spectral coverage of these data, and consequently, H II 152 was not included in our analysis here.

The Fe I and Fe II abundances were derived using the LTE stellar line analysis package MOOG (Sneden 1973) and model stellar atmospheres with convective overshoot interpolated from the standard ATLAS9 grids of R. Kurucz⁷. In previous analyses of open cluster dwarfs (e.g., Schuler et al. 2004, 2006a), we have shown that model atmospheres with convective overshoot produce consistent results as those without the overshoot approximation (NOVER). Presently, we have also tested for a subsample of our stars the more updated Kurucz models without overshoot that include the most recent opacity distribution functions (the ODFNEW models). The resulting [Fe I/H] and [Fe II/H] abundances are consistent with

those derived using the overshoot models; the differences range from 0 – 0.05 dex, with the ODFNEW-based abundances generally lower, similar to what was found previously for the NOVER models. The overshoot models used here are the same ones used by Schuler et al. (2004), from which the adopted stellar parameters are also taken. One exception is H II 298; for this star, we have used the updated dereddened $(B - V)_0$ color of King et al. (2010) to calculate new T_{eff} , $\log g$, and microturbulent velocity (ξ) values using the relations described in Schuler et al. (2004) and interpolate a new model from the Kurucz grids. The adopted stellar parameters for our sample are provided in Table 1.

3. RESULTS AND DISCUSSION

Line-by-line abundances derived for each of our Pleiades stars are listed in Tables 2 – 4, and the stellar mean abundances can be found in Table 5. The final mean abundances are given relative to solar values (Table 2) derived via an EW analysis of sky spectra obtained with the HET/HRS as part of our observational program. The relative abundances are determined on a line-by-line basis before the mean is taken; this strict line-by-line abundance analysis ensures that the final relative abundances are independent of the adopted oscillator strengths. The adopted solar parameters are included in Table 1. The mean $[\text{Fe I}/\text{H}]$ abundances and the differences in the mean $[\text{Fe II}/\text{H}]$ and $[\text{Fe I}/\text{H}]$ abundances ($\Delta\text{Fe} = [\text{Fe II}/\text{H}] - [\text{Fe I}/\text{H}]$) are plotted in Figure 1 along with errorbars for three representative stars– H II 263, H II 2284, and H II 3179– that run the T_{eff} range of our sample. The errorbars denote the total internal uncertainties (σ_{Total}) in the derived abundances. The σ_{Total} uncertainties are the quadratic sum of the abundance uncertainties resulting from errors in the adopted stellar parameters (Schuler et al. 2004) and the uncertainty in the mean abundance (Table 5). Abundance sensitivities to the stellar parameters were determined by individually altering effective temperature ($\Delta T_{\text{eff}} = \pm 150$ K), surface gravity ($\Delta \log g = \pm 0.30$ dex), and microturbulent velocity ($\Delta \xi = \pm 0.25$ km s^{−1}) and are given in Table 6. The σ_{Total} uncertainties in the Fe I abundances for the three representative stars are ± 0.03 , ± 0.05 , and ± 0.04 dex for H II 263, H II 2284, and H II 3179, respectively. For Fe II, the σ_{Total} uncertainties are ± 0.09 , ± 0.10 , and ± 0.08 , respectively. The errorbars for the $[\text{Fe II}/\text{H}] - [\text{Fe I}/\text{H}]$ abundances shown in Figure 1 represent the quadratically combined Fe I and Fe II individual σ_{Total} uncertainties.

The star-to-star $[\text{Fe I}/\text{H}]$ abundances fall within a narrow range of 0.11 dex and have a standard deviation in the mean of 0.04 dex. However, as can be seen in the left panel

⁷<http://kurucz.cfa.harvard.edu/grids.html>

of Figure 1, the $[\text{Fe I}/\text{H}]$ abundances of stars with $T_{\text{eff}} < 5400$ K are systematically higher than those of stars at higher T_{eff} . The discord is verified by the Spearman rank correlation coefficient ($r_s = -0.7612$) at the 99.97% confidence level. In the right panel of Figure 1, ΔFe abundances evince a dramatic increase at about the same T_{eff} , 5400 K. The ΔFe abundances result from large overabundances of Fe II among the cool dwarfs (Table 5), and the ΔFe vs. T_{eff} trend for the Pleiades is similar to those seen in M 34 (Schuler et al. 2003), the Hyades (Yong et al. 2004; Schuler et al. 2006a), and the UMa moving group (King & Schuler 2005).

3.1. Over-excitation/ionization

The increase in ΔFe with decreasing T_{eff} presented here resembles the trend of increasing Pleiades O abundances derived from the high-excitation O I triplet (Schuler et al. 2004). In particular, the increase in the O I triplet abundances also begins to become significant at approximately 5400 K. In Figure 2 ΔFe is plotted against the triplet abundances ($[\text{O}/\text{H}]_{\text{Trip}}$), and it is seen that a strong correlation between these two abundance anomalies does exist. According to the linear correlation coefficient ($r = 0.847$), ΔFe and $[\text{O}/\text{H}]_{\text{Trip}}$ are correlated at a greater than 99.9% confidence level. Also in Figure 2 we plot the *residuals* in the ΔFe and $[\text{O}/\text{H}]_{\text{Trip}}$ abundances. The residuals are differences between the observed abundances and T_{eff} -dependent fitted values calculated by fitting low-order (second or third) polynomials to the abundance versus T_{eff} relations (Figure 3); the fitted values are determined at each stellar T_{eff} . This procedure effectively removes the global mass dependence of the abundances so that the residuals are a measure of star-to-star abundance scatter at a given T_{eff} (King et al. 2000b). Similar to the ΔFe and $[\text{O}/\text{H}]_{\text{Trip}}$ abundances, their residuals are correlated, but at a slightly lower confidence level, 97% ($r = 0.589$). The strong relationship between the ΔFe and $[\text{O}/\text{H}]_{\text{Trip}}$ abundances and especially their residuals suggests the anomalous abundances share a common origin.

Inaccurate T_{eff} scales can give rise to T_{eff} -dependent abundance trends if the scales are in error in a systematic way. Pinsonneault et al. (2004) have raised concern as to the accuracy of color-temperature relations, like the one used for our Pleiades sample, arguing that disagreements between observed open cluster color-magnitude diagrams (CMDs) and theoretical isochrones based on color-temperature relations likely arise from systematic errors in the latter. An et al. (2007) are able to obtain near-perfect agreement between the observed CMDs of four nearby open clusters and isochrones using empirical corrections to the color-temperature relations as suggested by Pinsonneault et al. (2004). Inaccurate T_{eff} scales, however, do not appear to be at the root of the over-excitation/ionization effects observed among cool open cluster dwarfs. The Pleiades and Hyades $[\text{O}/\text{H}]_{\text{Trip}}$ abundances

of Schuler et al. (2004) and Schuler et al. (2006b), respectively, were derived using color-temperature relations *and* empirically corrected isochrones, and in both cases, the steep trends of increasing abundances with decreasing T_{eff} are present. The T_{eff} from the empirically corrected isochrones for the majority of dwarfs in both clusters are higher than those from the color-temperature relations, with the differences reaching a maximum of about 190 K. Temperature corrections of this magnitude also do not alleviate the large ΔFe abundances of the coolest stars in our sample. According to the abundance sensitivities given in Table 6, the T_{eff} of H II 263 ($T_{\text{eff}} = 5048$ K) would have to be higher by approximately 750 K in order to bring its Fe II and Fe I abundances into agreement; such errors in our adopted temperature scale are not expected (Pinsonneault et al. 2004). Furthermore, increasing the T_{eff} of H II 263 by 750 K would result in an 0.15 dex increase in its Fe I abundance and exacerbate the disagreement in the $[\text{Fe I/H}]$ abundances of the cool and warm dwarfs.

Whatever the cause of the anomalous ΔFe abundances, the phenomenon may also be affecting the $[\text{Fe I/H}]$ abundances of the Pleiads with $T_{\text{eff}} < 5400$ K. Schuler et al. (2003) found that the Si I abundances of the two coolest M 34 dwarfs (~ 4750 K) they analyzed are higher by about 0.1 dex than those of the rest of the sample; the Si I lines have excitation potentials of $\chi \sim 6$ eV. Similarly, Hyades Ni I abundances derived from lines with excitation potentials of approximately 4.25 eV increase with decreasing T_{eff} for dwarfs with $T_{\text{eff}} \leq 5100$ K (Schuler et al. 2006b). More interestingly, the Ni I abundances of a single cool Hyades dwarf ($T_{\text{eff}} = 4573$ K) derived from lines with excitation potentials of $\chi \approx 4.25$ eV were approximately 0.15 dex higher than the abundance derived from a line with a low excitation potential ($\chi = 1.83$ eV). For a warmer dwarf ($T_{\text{eff}} = 5978$ K), consistent abundances were obtained from all of the lines (please see Figure 7 of Schuler et al.). Similar behavior is not seen here in the line-by-line Fe I abundances of individual Pleiads (Figure 4). However, identifying such excitation potential-related effects for a given cool Pleiades star is difficult, because the standard deviation, a measure of the dispersion in the line-by-line abundances, in the mean $[\text{Fe I/H}]$ abundance of each Pleiad ranges from 0.04 to 0.13 dex and has an average of 0.07 dex. This is of the order of the effect seen among the cooler stars in M 34 and Hyades dwarfs, for which the effect is expected to be more severe. Thus, a direct connection between the heightened mean $[\text{Fe I/H}]$ abundances and the over-excitation phenomenon cannot be made, but nonetheless, the fact that the $[\text{Fe I/H}]$ abundances increase at the same T_{eff} as ΔFe and the O I triplet abundances is intriguing and suggests that they all are the result of the same effect.

3.2. ΔFe and Stellar Activity

Intercluster comparisons of the cool cluster dwarf abundance anomalies can provide valuable insight into the nature of the over-excitation/ionization effects by potentially linking differences in abundance trend morphologies to differences in the physical characteristics of the clusters, such as age and metallicity. In Figure 5 the Pleiades ΔFe values along with those of the Hyades from Schuler et al. (2006a) are plotted versus T_{eff} . The ΔFe abundances of these two clusters follow the same trend down to a T_{eff} of about 5200 K, below which the Pleiades abundances clearly diverge. Similar behavior is seen in the O I abundances of dwarfs in the Hyades, Pleiades and UMa moving group (Schuler et al. 2006b). The O I abundances of stars in all three associations increase at similar rates down to a T_{eff} of about 5200 K, below which the Pleiades trend becomes much steeper than both of those of the Hyades and UMa, which continue to track each other. The UMa moving group has an age that is comparable to that of the Hyades (King & Schuler 2005) and a metallicity that is lower than both Pleiades and Hyades (Boesgaard & Friel 1990). The divergence of the Pleiades O I triplet abundances from those of both the Hyades and UMa suggests that the abundance trends may undergo an age-related diminution; the ΔFe abundances of the Pleiades and Hyades are consistent with this conclusion.

Chromospheric emission and photospheric spots are two age-related phenomena that have been discussed in the literature as possible sources of the observed over-excitation/ionization effects. Schuler et al. (2006b) demonstrated using multicomponent model atmospheres that spotted photospheres can plausibly account for the O I triplet abundances of the cool Hyades dwarfs. Results from efforts investigating a possible connection between chromospheric activity and the anomalous O I triplet abundances of cool dwarfs, on the other hand, have been mixed. No correlation between $H\alpha$ and Ca II infrared triplet emission measures and O I triplet abundances of Pleiades dwarfs nor M 34 dwarfs exists (Schuler et al. 2004). However, Morel & Micela (2004) found a strong correlation between X-ray activity indicators and Pleiades triplet abundances taken from the literature. There is no correlation between Ca II H+K emission indicators and the Hyades O I triplet abundances (Schuler et al. 2006b). For the young cluster IC 4665, Shen et al. (2007) show that the O I abundances of the cool dwarfs are highly correlated with both $H\alpha$ and Ca II infrared triplet emission indicators. It is important to note that Shen et al. is the only of these studies that derived the O I abundances and chromospheric emission levels from the same spectra. For the others, the measurements were made or taken from different sources, and thus the actual chromospheric emission level may have been different when the spectral lines were formed.

As can be seen from these various studies, it is not clear if there is a connection between chromospheric emission and the over-excitation of O I. Furthermore, chromospheric emission

is often correlated with T_{eff} , so any correlation between chromospheric emission and O I abundances may be masking some other T_{eff} -dependent effect (Schuler et al. 2006b). Using the chromospheric emission data from Soderblom et al. (1993), we have plotted the Pleiades ΔFe versus Ca II infrared triplet chromospheric emission indicators ($\log R'_{\text{IRT}}$ ⁸) in Figure 6 and find a correlation that is significant at greater than the 99.9% confidence level according to the linear correlation coefficient ($r = 0.893$). A similar correlation is found for the H α chromospheric emission ($\log R'_{\text{H}\alpha}$). These correlations, while suggestive of a connection between chromospheric emission and the over-ionization of Fe, should be viewed with caution, because $\log R'_{\text{H}\alpha}$ and $\log R'_{\text{IRT}}$ are also correlated with T_{eff} at approximately the 93% and 98% confidence levels. This degeneracy makes it unclear if the ΔFe abundances, like those of O I, are affected by chromospheric emission or some other T_{eff} -dependent effect.

More importantly, residual ΔFe abundances and residual chromospheric emission indicators (calculated in the same manner as the abundance residuals, i.e., they are the differences between observed and T_{eff} -dependent fitted values; please see Figure 3) are correlated at the 93% and 99.9% confidence levels for H α and Ca II infrared triplet, respectively (Figure 6). These relationships are more indicative of a true correlation between chromospheric emission and the over-ionization of Fe. We remind the reader, however, that the ΔFe abundances and chromospheric emission indicators were not measured using the same spectra and are thus not cotemporal.

3.3. ΔFe Residuals and the Pleiades Li Dispersion

King et al. (2010) have used the same HET/HRS spectra analyzed here to examine the long-standing problem of the large Li abundance dispersion observed among cool Pleiades dwarfs. These authors find evidence that at least a portion of the dispersion is due to real Li depletion and suggest that the differential depletion may be a consequence of stellar radius modulations induced by surface magnetic activity, i.e., spots, during pre-MS evolution. It is also suggested that such spot-induced effects could be related to the over-excitation/ionization effects observed today.

ΔFe residuals are plotted versus Li abundance residuals in Figure 7. Li abundances are derived from $\lambda 6707$ Li I line strengths and are taken from King et al. (2010). The ΔFe and Li residuals relation has a correlation coefficient of $r = 0.46$, corresponding to a $\sim 91\%$ confidence level. While only marginally significant at best, the mild correlation still means

⁸The R' index is the ratio of the flux in the line core (Ca II infrared triplet or H α) to the star's bolometric flux (Noyes et al. 1984).

that a substantial fraction (nearly-half) of the variance in ΔFe is related to that in Li. The abstract picture painted by this result is consistent with the conjecture presented by King et al. (2010): the considerable Li abundance dispersion in cool Pleiades dwarfs has a real pre-MS depletion component, a portion of which may be driven by the same mechanism (the influence of spots) but perhaps by different physics (the influence on stellar structure versus the influence on line formation in addition to or independent of stellar structure) that is also possibly responsible for the Fe II versus Fe I differences seen in these stars. This would explain the overlap in the variance of Pleiades ΔFe and Li abundances but allow for only marginally significant present-day correlations between these observables. Observational tests, using the same type of Pleiades spectroscopic/photometric monitoring program proposed in the Conclusions section below, of this possibility are discussed in King et al. (2010).

3.4. Pleiades Cluster Metallicity

The mean abundance of the Pleiades stars above 5400 K derived from Fe I lines is $[\text{Fe}/\text{H}] = +0.01 \pm 0.02$ (uncertainty in the mean) compared to $[\text{Fe}/\text{H}] = +0.07 \pm 0.01$ (uncertainty in the mean) for stars below 5400 K. While a direct connection between the high $[\text{Fe I}/\text{H}]$ abundances and the over-excitation effects manifested in the $[\text{O}/\text{H}]_{\text{Trip}}$ abundances of cool open cluster dwarfs cannot be made here, the similarities are suggestive and raise doubt as to the accuracy of the cool star $[\text{Fe I}/\text{H}]$ abundances. For this reason, and because of the anomalously high Fe II abundances, we feel that the mean cluster metallicity is best estimated by the $[\text{Fe I}/\text{H}]$ abundances of the warmer stars only, and adopt the value of $[\text{Fe}/\text{H}] = +0.01 \pm 0.02$ for the Pleiades.

The Pleiades is one of the most well studied Galactic open clusters, and Fe abundances of member F, G, and K dwarfs have been derived using high-resolution spectroscopy by a handful of groups, which are summarized in Table 7. Cayrel et al. (1988) found a mean abundance of $[\text{Fe}/\text{H}] = +0.13$ from one F and three G dwarfs, though the abundances are characterized by a large dispersion (0.02 – 0.26 dex). The spectra of three of the stars have S/N ratios of ~ 40 . In the same year, Boesgaard et al. (1988) report a cluster mean abundance of $[\text{Fe}/\text{H}] = +0.003 \pm 0.054$ for 13 F stars that have standard deviations in their individual $[\text{Fe}/\text{H}]$ abundances ≤ 0.10 dex; the mean abundance of their entire 17 star sample is $[\text{Fe}/\text{H}] = -0.03$. Subsequent to that, Boesgaard (1989) and Boesgaard & Friel (1990) find similar values, $[\text{Fe}/\text{H}] = +0.02$ and -0.02 , respectively. King et al. (2000a) derived the abundances of two cool Pleiades K dwarfs and obtained a mean abundance of $[\text{Fe}/\text{H}] = +0.06$ from an analysis of Fe I lines. This value is almost identical to that of the stars

with $T_{\text{eff}} < 5400$ K in our sample, and we suspect that the abundances of the two K dwarfs from King et al. are similarly suspect. However, Gebran & Monier (2008) also derived a mean abundance of $[\text{Fe}/\text{H}] = +0.06$ but for five F dwarfs. These authors noted that their result is slightly larger than that of Boesgaard & Friel (1990) and suggested differences in the analyses, i.e., spectral lines used and adopted stellar parameters, as a possible cause. Finally, Funayama et al. (2009) have recently reported a cluster abundance of $[\text{Fe}/\text{H}] = +0.03 \pm 0.05$ based on 22 A, F, and G stars.

Excluding the results of Cayrel et al. (1988) due to poor data quality and those of King et al. (2000a) due to the uncertainty in the abundances of the two cool K dwarfs studied, the mean Pleiades cluster abundance of the six remaining studies, including ours, is $[\text{Fe}/\text{H}] = +0.01$ with a standard deviation of $\sigma_{\text{s.d.}} = 0.03$. This is identical to the value from the five stars with $T_{\text{eff}} > 5400$ K in our sample, and by our assessment, represents the best estimate of the Pleiades cluster metallicity.

4. CONCLUSIONS

We have derived Fe abundances via an EW analysis of Fe I and Fe II lines in high-resolution and moderate-S/N spectra of 16 MS dwarfs in the Pleiades open cluster. The $[\text{Fe II}/\text{H}]$ abundances increase dramatically relative to $[\text{Fe I}/\text{H}]$ at T_{eff} below 5400 K, with the difference reaching over 0.8 dex in the coolest stars. This behavior is akin to what is seen in M 34, the Hyades, and the UMa moving group. Comparison of the ΔFe abundance patterns in the Pleiades and Hyades, as well as the $[\text{O}/\text{H}]_{\text{Trip}}$ abundances in the Pleiades, Hyades, and UMa moving group, suggests that the trends may relax with age, though metallicity may yet prove to be a factor. Abundances of cool dwarfs in additional open clusters or other stellar associations, especially those older than the Hyades, are needed to determine if either age or metallicity are related to these anomalous abundances.

The $[\text{Fe I}/\text{H}]$ abundances are also higher in Pleiads below 5400 K, but they show no evidence of an increase with decreasing T_{eff} . The inability to attribute the high $[\text{Fe I}/\text{H}]$ abundances of the cool stars to the over-excitation effects illustrates the difficulty of quantifying this phenomenon. With lines of exceptionally high excitation potential such as the O I triplet, the over-excitation effect is clearly seen (e.g., Schuler et al. 2006b; Shen et al. 2007), but for lines with excitation potentials $\lesssim 5$ eV, the effect is more difficult to pinpoint. Our Fe I linelist includes transitions ranging in excitation potential from 2.18 to 5.10 eV, but for the individual Pleiades stars, no increase in the line-by-line abundances as a function of excitation potential, like that seen in Ni I abundances of cool Hyades dwarfs ($1.83 \text{ eV} \leq \chi \leq 4.42 \text{ eV}$; Schuler et al. 2006a), is evident (Figure 4). Line-to-line sensitivities to

the over-excitation/ionization effects have yet to be clearly delineated, and it needs to be determined if there is an excitation potential threshold above which the abundances derived from these lines become enhanced by these effects. Similarly, it needs to be determined if there is an excitation potential threshold *below* which the opposite occurs, the abundances derived from the low-excitation lines are lower due to these effects. Such behavior would be expected if the overabundances of high-excitation (singly ionized) lines are due to the overpopulation of high-excitation (singly ionized) electronic states at the expense of depopulating low-excitation states. Whether or not the over-excitation effects impact the spectroscopic derivation of stellar parameters (T_{eff} , $\log g$, and ξ), an approach not adopted here, also needs to be determined. Future investigations of these effects will require high-quality high-resolution spectroscopy so that accurate line-by-line abundances can be derived, even from features of just a few mÅ in strength.

A strong correlation between the ΔFe and $[\text{O}/\text{H}]_{\text{Trip}}$ abundances of the Pleiades dwarfs is evident in Figure 2, suggesting that the over-excitation/ionization effects share a common cause or origin. Chromospheric emission and photospheric spots have been shown to be promising culprits, but to this point, the data are inconclusive. Whereas strong correlations between the Pleiades ΔFe and chromospheric emission indicators and their residuals exist, they do not exist between $[\text{O}/\text{H}]_{\text{Trip}}$ and chromospheric emission. These contradictory results complicate the interpretation of the observed over-excitation/ionization effects and will have to be addressed by future studies. Also, comparing abundances and chromospheric emission indicators measured using different spectra may not provide an accurate test of a true correlation because of potential temporal changes in chromospheric activity levels. Future investigations into the over-excitation/ionization effects in cool open cluster dwarfs should make every effort to derive chromospheric activity levels from the same spectra so that any possible relation between the two can be more definitively delineated.

Determining the influence of photospheric spots on abundance derivations is more arduous. Multicomponent model atmospheres- simulating photospheres with different areal coverages of hot, cool, and quiescent spots- have been shown to be able to reproduce the measured EWs of the O I triplet in a sample of Hyades stars, but, while such exercises are useful and demonstrate the plausibility of the photospheric spot hypothesis, the results are only suggestive. Observationally, a simultaneous photometric and spectroscopic monitoring program could be used to identify any correlated changes in spot coverage and spectral line strengths. Such observational constraints would be helpful to determine if spotted photospheres affect high-resolution abundance derivations. Despite the challenges, the possible connection between spots, over-excitation/ionization effects, and pre-MS Li depletion should provide sufficient motivation for future efforts.

A final conclusion that can be drawn from this study is that those carrying out spectroscopic abundance analyses of open clusters should heed caution when their samples include cool dwarfs, particularly those with $T_{\text{eff}} < 5400$ K. Including the abundances of these stars may skew cluster mean abundances. A similar caution may be needed for those studying cool MS dwarfs in the disk field, as well. Further investigations into the sensitivity of the over-excitation/ionization effects to excitation potential, first ionization potential, stellar age, and stellar metallicity are needed in order to identify the extent and ubiquity of these effects.

A.L.P. gratefully acknowledges her support for summer research from the National Science Foundation through their Research Experience for Undergraduates program at Cerro Tololo Inter-American Observatory (grant AST-0647604). A.L.P. also thanks the C.V. Starr-Middlebury School in Latin America for additional support. S.C.S. is grateful for support provided by the NOAO Leo Goldberg Fellowship; NOAO is operated by the Association of Universities for Research Astronomy, Inc., under a cooperative agreement with the National Science Foundation. J.R.K. gratefully acknowledges support for this work by grants AST 00-86576 and AST 02-39518 to J.R.K. from the National Science Foundation and by a generous grant from the Charles Curry Foundation to Clemson University.

Facilities: HET (HRS)

REFERENCES

- Allende Prieto, C., Barklem, P. S., Lambert, D. L., & Cunha, K. 2004, *A&A*, 420, 183
- An, D., Terndrup, D. M., Pinsonneault, M. H., Paulson, D. B., Hanson, R. B., & Stauffer, J. R. 2007, *ApJ*, 655, 233
- Asplund, M. 2005, *ARA&A*, 43, 481
- Boesgaard, A. M. 1989, *ApJ*, 336, 798
- Boesgaard, A. M., Budge, K. G., & Ramsay, M. E. 1988, *ApJ*, 327, 389
- Boesgaard, A. M. & Friel, E. D. 1990, *ApJ*, 351, 467
- Castelli, F. & Kurucz, R. L. 2004, *arXiv:astro-ph/0405087*
- Cayrel, R., Cayrel de Strobel, G., & Campbell, B. 1988, *The Impact of Very High S/N Spectroscopy on Stellar Physics*, 132, 449
- Chen, Y. Q., Zhao, G., Izumiura, H., Zhao, J. K., Liu, Y. J., Honda, S., & Ohkubo, M. 2008, *AJ*, 135, 618
- D’Orazi, V. & Randich, S. 2009, *A&A*, 501, 553
- Fabbian, D., Asplund, M., Barklem, P. S., Carlsson, M., & Kiselman, D. 2009, *A&A*, 500, 1221
- Feltzing, S. & Gustafsson, B. 1998, *A&AS*, 129, 237
- Fitzpatrick, M. J. & Sneden, C. 1987, *BAAS*, 19, 1129
- Funayama, H., Itoh, Y., Oasa, Y., Toyota, E., Hashimoto, O., & Mukai, T. 2009, *PASJ*, 61, 930
- Gebran, M. & Monier, R. 2008, *A&A*, 483, 567
- King, J. R., Krishnamurthi, A., & Pinsonneault, M. H. 2000b, *AJ*, 119, 859
- King, J. R. & Schuler, S. C. 2005, *PASP*, 117, 911
- King, J.R., Schuler, S.C., Hobbs, L.M., & Pinsonneault, M.H. 2010, *ApJ*, 710, 1610
- King, J. R., Soderblom, D. R., Fischer, D., & Jones, B. F. 2000a, *ApJ*, 533, 944
- Kroupa, P. 2002, *Science*, 295, 82

- Kupka, F., Piskunov, N., Ryabchikova, T. A., Stempels, H. C., & Weiss, W. W. 1999, *A&AS*, 138, 119
- Morel, T. & Micela, G. 2004, *A&A*, 423, 677
- Noyes, R. W., Hartmann, L. W., Baliunas, S. L., Duncan, D. K., & Vaughan, A. H. 1984, *ApJ*, 279, 763
- Oinas, V. 1974, *ApJS*, 27, 405
- Pinsonneault, M. H., Terndrup, D. M., Hanson, R. B., & Stauffer, J. R. 2004, *ApJ*, 600, 946
- Piskunov, N. E., Kupka, F., Ryabchikova, T. A., Weiss, W. W., & Jeffery, C. S. 1995, *A&AS*, 112, 525
- Ramírez, I., Allende Prieto, C., & Lambert, D. L. 2007, *A&A*, 465, 271
- Ryabchikova, T. A., Piskunov, N. E., Stempels, H. C., Kupka, F., & Weiss, W. W. 1999, *Phys. Scr.*, T83, 162
- Schuler, S. C., Hatzes, A. P., King, J. R., Kürster, M., & The, L.-S. 2006a, *AJ*, 131, 1057
- Schuler, S. C., King, J. R., Fischer, D. A., Soderblom, D. R., & Jones, B. F. 2003, *AJ*, 125, 2085
- Schuler, S. C., King, J. R., Hobbs, L. M., & Pinsonneault, M. H. 2004, *ApJ*, 602, L117
- Schuler, S. C., King, J. R., Terndrup, D. M., Pinsonneault, M. H., Murray, N., & Hobbs, L. M. 2006b, *ApJ*, 636, 432
- Shen, Z.-X., Jones, B., Lin, D. N. C., Liu, X.-W., & Li, S.-L. 2005, *ApJ*, 635, 608
- Shen, Z.-X., Liu, X.-W., Zhang, H.-W., Jones, B., & Lin, D. N. C. 2007, *ApJ*, 660, 712
- Snedden, C. 1973, *ApJ*, 184, 839
- Soderblom, D. R., Jones, B. F., Balachandran, S., Stauffer, J. R., Duncan, D. K., Fedele, S. B., & Hudon, J. D. 1993, *AJ*, 106, 1059
- Takeda, Y. 2003, *A&A*, 402, 343
- Yong, D., Lambert, D. L., Allende Prieto, C., & Paulson, D. B. 2004, *ApJ*, 603, 697

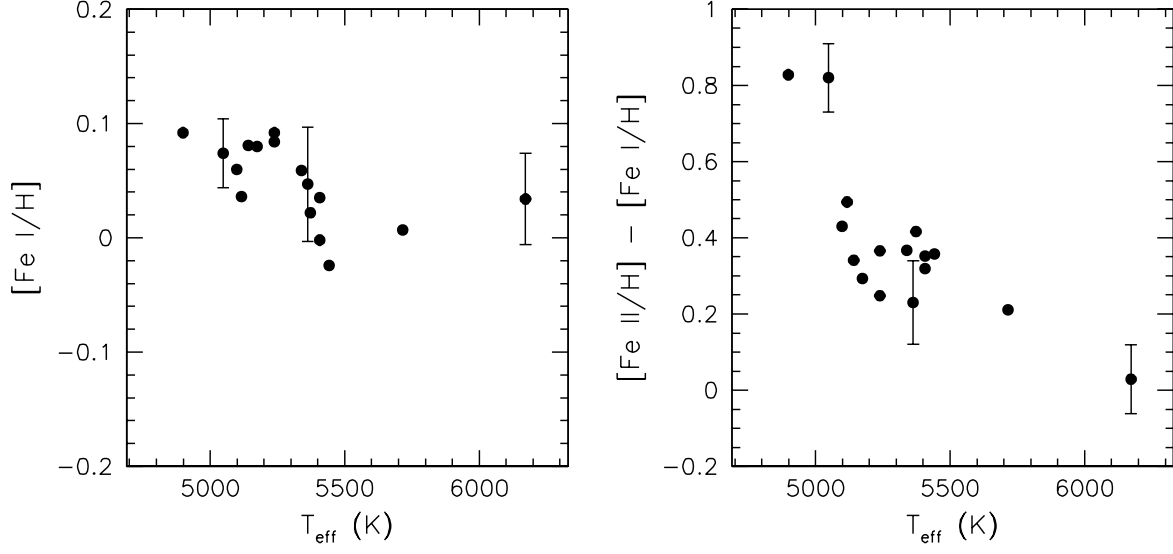


Fig. 1.— Left: Fe abundances derived from Fe I lines vs T_{eff} . Errorbars for three representative stars- H II 263, H II 2284, and H II 3179- are shown and illustrate the total internal abundance uncertainties, as described in the text. Right: ΔFe vs T_{eff} . The errorbars for the three representative stars depict the quadratically combined Fe I and Fe II individual total internal uncertainties.

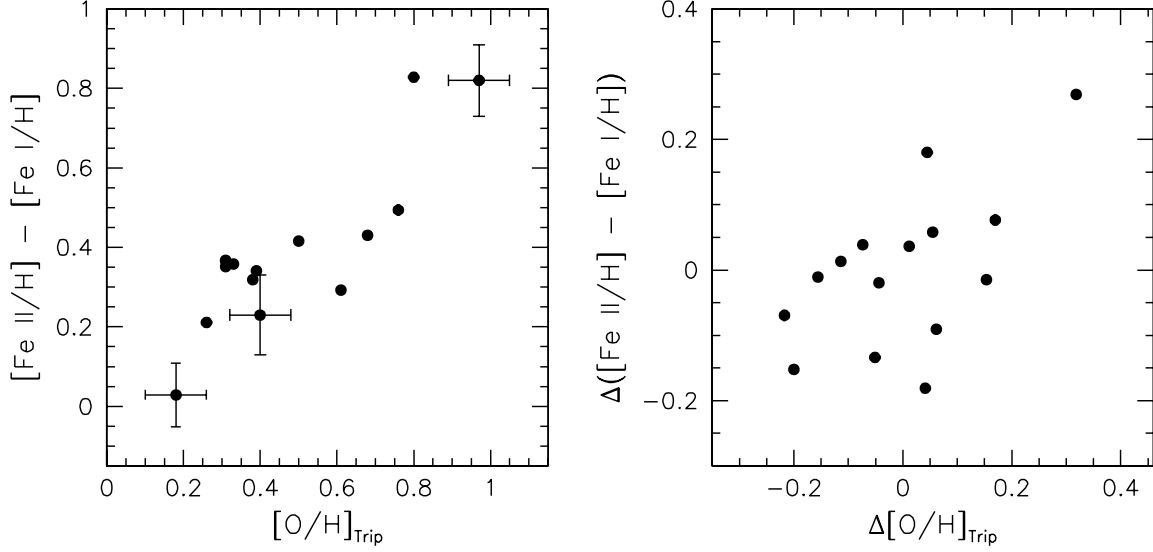


Fig. 2.— Left: ΔFe plotted against O abundances derived from the high-excitation O I triplet. The $[\text{O}/\text{H}]_{\text{Trip}}$ abundances and typical uncertainties (shown as the horizontal errorbars) are from Schuler et al. (2004). The vertical errorbars are those shown in the right panel of Figure 1. ΔFe is correlated with $[\text{O}/\text{H}]_{\text{Trip}}$ at greater than the 99.9% confidence level according to the linear correlation coefficient ($r = 0.847$). Right: ΔFe residuals vs O abundance residuals. The residuals are the differences in observed and T_{eff} -dependent fitted values. The residuals are correlated at a 97% confidence level ($r = 0.589$).

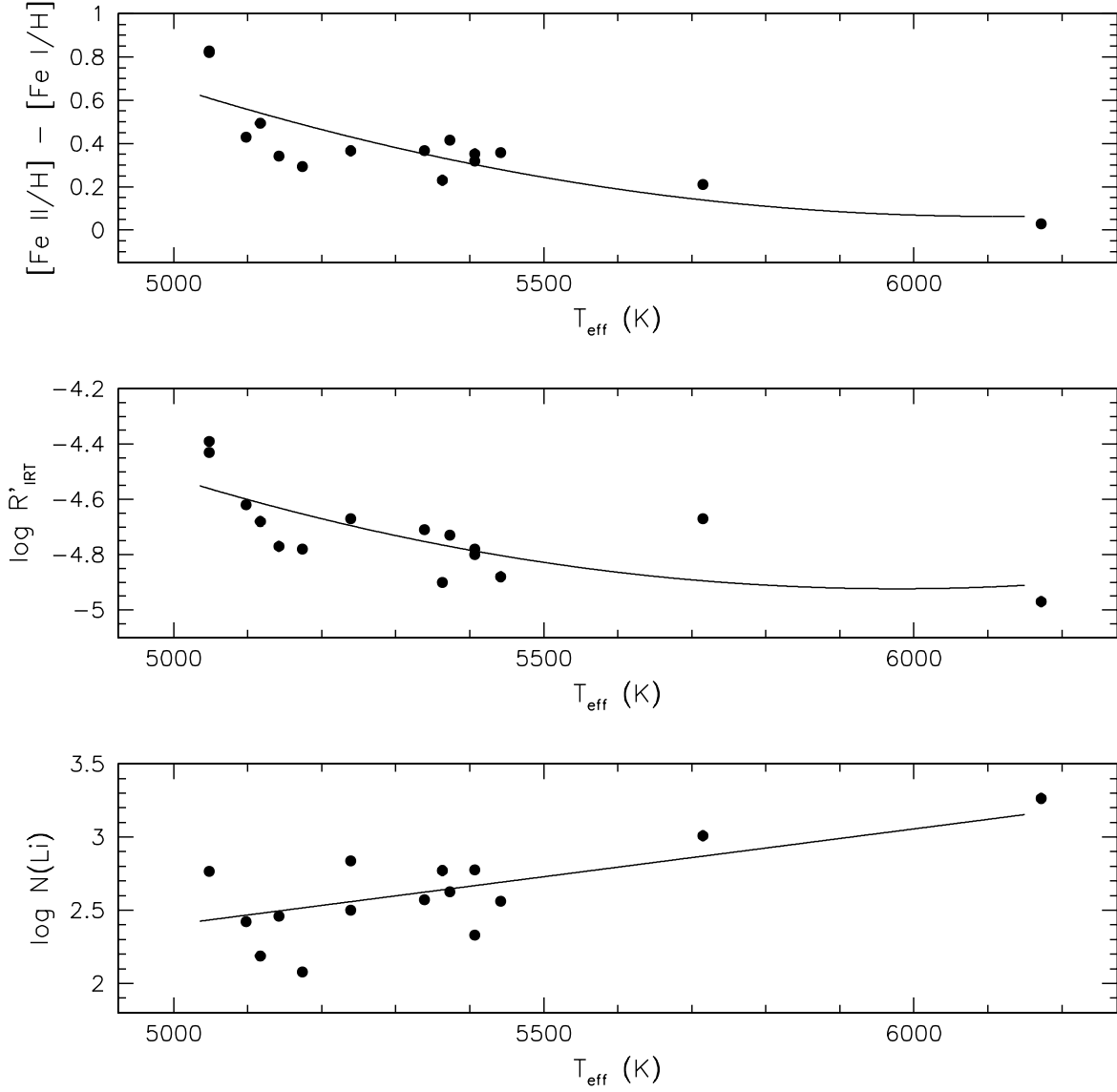


Fig. 3.— Polynomial fits (solid lines) to ΔFe , $\log R'_{\text{IRT}}$, and Li abundance versus T_{eff} relations for the Pleiades dwarfs. The fits are used to calculate residuals- differences between observed and fitted values- in the abundances and chromospheric activity indicators for each star.

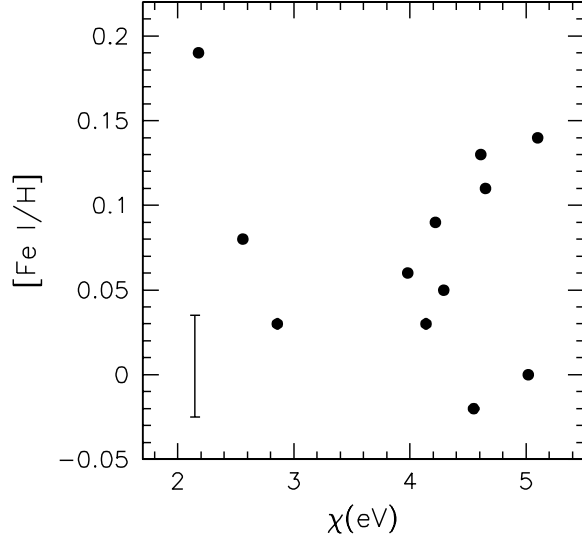


Fig. 4.— Line-by-line Fe abundances of H II 263 derived from Fe I lines vs excitation potential. There is no trend in the abundances as a function of excitation potential. The standard deviation of the abundances is $\sigma_{s.d.} = 0.06$ and is shown as the errorbar in the lower right hand corner.

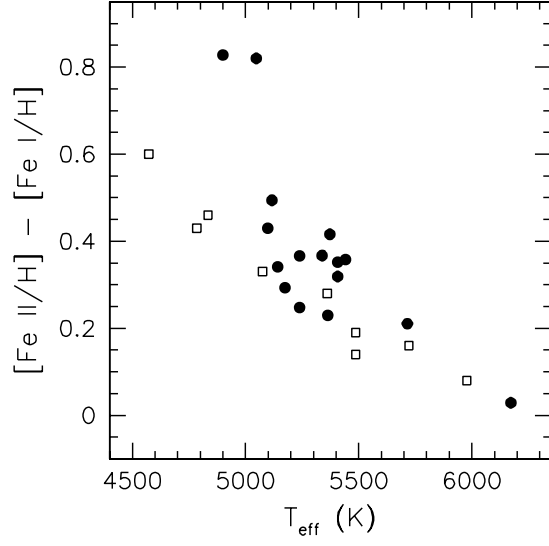


Fig. 5.— ΔFe for the Pleiades (closed circles) and the Hyades (open squares) as a function of T_{eff} . The Hyades data are from Schuler et al. (2006a).

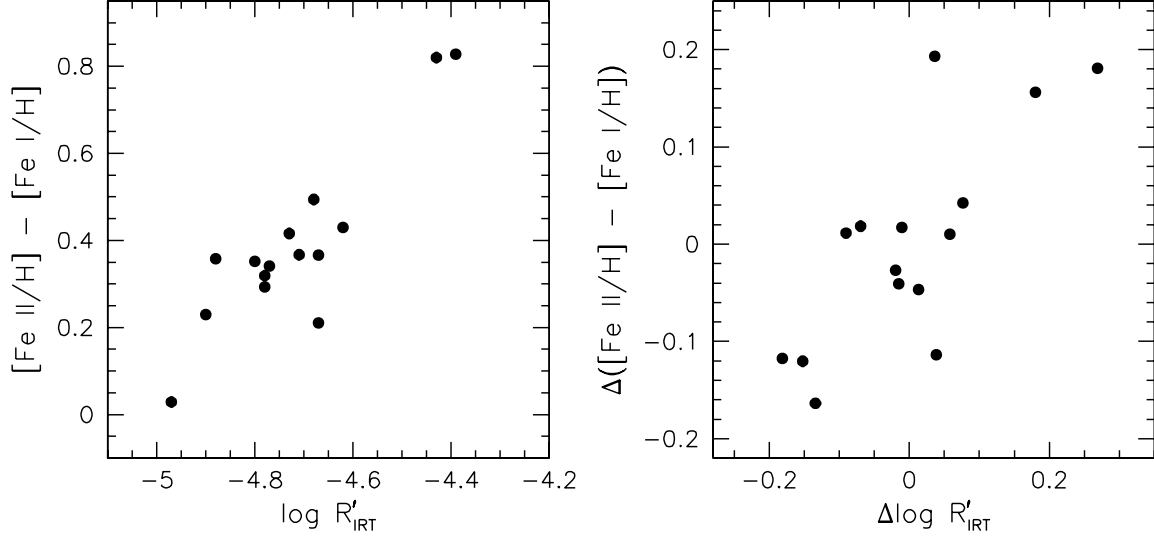


Fig. 6.— Left: ΔFe vs Ca II infrared triplet chromospheric emission indicator. According to the linear correlation coefficient ($r = 0.893$), the ΔFe abundances are correlated with the Ca II chromospheric emission with greater than 99.9% confidence. The chromospheric emission data are taken from Soderblom et al. (1993). Right: ΔFe residuals vs residuals in Ca II infrared triplet chromospheric emission indicators. The quantities are correlated at the 99.9% confidence level ($r = 0.766$).

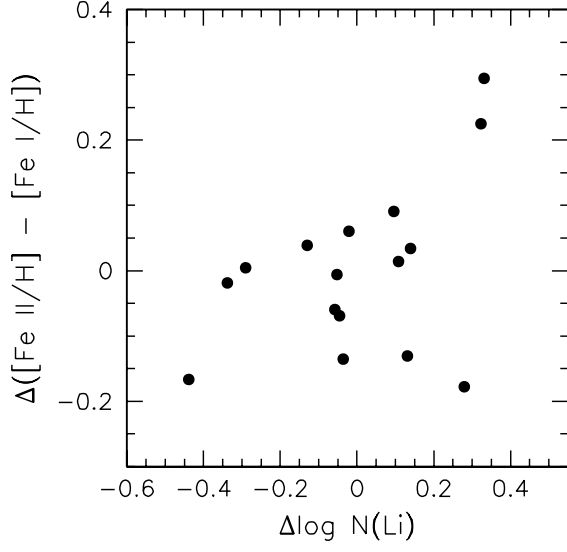


Fig. 7.— ΔFe residuals vs Li I abundance residuals. The Li I abundances are from King et al. (2010). The linear correlation coefficient ($r = 0.456$) is marginally significant at the $\sim 91\%$ confidence level.

Table 1. Stellar Parameters

Star	$(B - V)_o$ (mag)	T_{eff} (K)	$\log g$ (cgs)	ξ (km s ⁻¹)
HII 0152	0.65	5715	4.55	0.96
HII 0193	0.75	5339	4.61	0.58
HII 0250	0.65	5715	4.55	0.96
HII 0263	0.84	5048	4.64	0.30
HII 0298	0.89	4899	4.66	0.16
HII 0571	0.75	5373	4.60	0.61
HII 0746	0.73	5407	4.60	0.65
HII 0916	0.82	5098	4.64	0.35
HII 1593	0.73	5407	4.60	0.65
HII 2126	0.81	5142	4.63	0.39
HII 2284	0.74	5363	4.61	0.60
HII 2311	0.78	5239	4.62	0.48
HII 2366	0.78	5239	4.62	0.48
HII 2406	0.72	5442	4.59	0.68
HII 2462	0.80	5174	4.63	0.42
HII 2880	0.82	5117	4.64	0.37
HII 3179	0.53	6172	4.48	1.42
Sun	5777	4.44	1.38

Table 2. Equivalent Widths and Abundances

	λ	χ		Sun		H II 193		H II 250		H II 263		H II 298		H II 571	
Ion	(Å)	(eV)	$\log gf$	EW	$\log N$	EW	$\log N$	EW	$\log N$	EW	$\log N$	EW	$\log N$	EW	$\log N$
Fe I	5793.92	4.22	-1.70	33.9	7.52	46.0	7.63	37.0	7.59	47.5	7.61	45.4	7.56	39.3	7.51
	5856.10	4.29	-1.64	36.6	7.57	42.1	7.56	30.8	7.46	47.8	7.62	51.1	7.67	43.0	7.59
	5927.80	4.65	-1.09	45.7	7.52	54.0	7.58	41.5	7.46	60.3	7.63	63.9	7.67	56.5	7.63
	6089.57	5.02	-0.94	41.8	7.64	47.1	7.63	35.3	7.52	49.5	7.64	56.6	7.74	43.0	7.57
	6093.65	4.61	-1.50	32.0	7.63	39.6	7.67	30.4	7.60	45.9	7.76	42.5	7.69	39.4	7.68
	6096.67	3.98	-1.93	41.2	7.64	52.8	7.75	42.4	7.68	52.9	7.70	55.1	7.72	49.2	7.69
	6151.62	2.18	-3.29	52.5	7.45	66.5	7.58	53.6	7.50	76.0	7.64	61.4	7.48
	6165.36	4.14	-1.47	48.3	7.46	58.3	7.56	47.2	7.47	58.1	7.49	57.6	7.47	53.0	7.46
	6270.23	2.86	-2.71	56.2	7.59	70.8	7.77	57.6	7.67	68.8	7.62	75.3	7.69
	6627.56	4.55	-1.68	30.9	7.71	30.6	7.59	30.0	7.69	37.0	7.69	39.1	7.74	36.6	7.73
	6806.86	2.73	-3.21	36.4	7.57	53.1	7.72	37.8	7.60	47.1	7.61
	6839.84	2.56	-3.45	37.2	7.65	35.8	7.62	58.4	7.76	38.5	7.48
	6842.69	4.64	-1.32	41.8	7.64	43.5	7.68	44.1	7.60
	6857.25	4.07	-2.15	23.4	7.54	35.0	7.66	23.8	7.54	37.1	7.66	28.5	7.52
	6861.94	2.42	-3.89	21.5	7.61	42.5	7.69	32.5	7.63
	6862.50	4.56	-1.57	29.9	7.58	45.9	7.76	40.2	7.69
	7284.84	4.14	-1.75	38.8	7.51	46.0	7.66	57.9	7.64	51.0	7.65
	7461.53	2.56	-3.58	29.2	7.59	37.4	7.53	48.5	7.67	50.4	7.68	42.0	7.64
	7547.90	5.10	-1.35	22.6	7.67	27.5	7.70	33.3	7.81	29.4	7.74
Fe II	5264.81	3.23	-3.13	43.8	7.40	42.1	7.82	42.9	7.54	49.9	8.31	44.0	7.84
	5414.05	3.22	-3.65	30.7	7.61
	5425.25	3.20	-3.39	39.4	7.53	39.7	7.99	40.8	7.71	41.3	8.32	39.6	8.45	40.5	7.97
	6084.10	3.20	-3.88	22.0	7.59
	6247.56	3.89	-2.44	52.6	7.49	47.4	7.92	56.8	7.77	52.5	8.37	47.2	8.43	50.5	7.96
	6432.68	2.89	-3.69	42.0	7.55	39.8	7.96	41.8	7.70	48.1	8.48	41.5	8.50	37.2	7.86
	6456.39	3.90	-2.19	63.4	7.45	55.7	7.86	69.6	7.79	67.1	8.41	53.0	8.32	63.0	7.98

Table 2—Continued

	λ	χ		Sun		H II 193		H II 250		H II 263		H II 298		H II 571	
Ion	(Å)	(eV)	$\log gf$	EW	$\log N$	EW	$\log N$	EW	$\log N$	EW	$\log N$	EW	$\log N$	EW	$\log N$

Table 3. Equivalent Widths and Abundances

Ion	λ	χ	$\log gf$	H II 746		H II 916		H II 1593		H II 2126		H II 2284		H II 2311	
	(Å)	(eV)		EW	$\log N$	EW	$\log N$	EW	$\log N$	EW	$\log N$	EW	$\log N$	EW	$\log N$
Fe I	5793.92	4.22	-1.70	40.4	7.54	48.0	7.62	40.5	7.54	49.5	7.66	48.2	7.69	46.5	7.62
	5856.10	4.29	-1.64	40.9	7.56	46.7	7.61	40.9	7.56	49.4	7.66	41.0	7.23	44.3	7.58
	5927.80	4.65	-1.09	53.0	7.57	58.0	7.60	51.2	7.54	60.5	7.64	53.2	7.56	55.5	7.58
	6089.57	5.02	-0.94	42.4	7.56	49.5	7.64	41.6	7.55	47.0	7.60	46.7	7.63	54.4	7.73
	6093.65	4.61	-1.50	38.5	7.67	41.0	7.67	39.0	7.68	40.7	7.66	40.1	7.69
	6096.67	3.98	-1.93	51.0	7.74	54.0	7.72	46.8	7.65	55.2	7.76	56.1	7.83	51.3	7.70
	6151.62	2.18	-3.29	63.9	7.55	69.5	7.53	61.7	7.50	80.0	7.75	70.9	7.68	72.9	7.66
	6165.36	4.14	-1.47	53.5	7.48	62.3	7.57	49.9	7.41	56.6	7.48	51.6	7.43	57.0	7.51
	6270.23	2.86	-2.71	63.5	7.64	67.0	7.60	64.2	7.66	73.1	7.73	71.2	7.54	69.5	7.70
	6627.56	4.55	-1.68	35.1	7.70	41.1	7.78	35.1	7.70	38.6	7.73	42.2	7.84	39.6	7.56
	6806.86	2.73	-3.21	46.3	7.60	55.1	7.68	44.6	7.57	58.7	7.77	49.8	7.66	53.7	7.70
	6839.84	2.56	-3.45	42.5	7.58	52.0	7.67	39.1	7.51	46.9	7.57	43.8	7.59	49.6	7.66
	6842.69	4.64	-1.32	51.0	7.73	48.5	7.64	48.6	7.69	49.9	7.70	48.1	7.65
	6857.25	4.07	-2.15	33.2	7.64	33.0	7.57	31.1	7.59	35.3	7.63	30.2	7.56	37.6	7.69
	6861.94	2.42	-3.89	26.6	7.51	33.4	7.53	26.3	7.50	32.0	7.61
	6862.50	4.56	-1.57	36.4	7.62	42.5	7.70	35.0	7.59	43.0	7.74	40.3	7.66
	7284.84	4.14	-1.75	50.8	7.65	55.6	7.69	48.8	7.61	48.8	7.60
	7461.53	2.56	-3.58	45.0	7.72	48.4	7.68	36.6	7.54	42.2	7.55	45.9	7.72	47.6	7.71
	7547.90	5.10	-1.35	31.7	7.78	27.0	7.69	31.7	7.78
Fe II	5264.81	3.23	-3.13	37.7	7.64	36.6	7.91	41.9	7.76	32.7	7.75	34.7	7.60	37.7	7.79
	5414.05	3.22	-3.65	27.0	7.98
	5425.25	3.20	-3.39	37.3	7.86	38.0	7.88	32.1	7.96	39.6	7.96	37.3	8.01
	6084.10	3.20	-3.88	21.3	7.88	14.5	7.66
	6247.56	3.89	-2.44	51.0	7.93	38.4	7.96	48.5	7.87	40.7	7.97	44.0	7.81	43.8	7.93
	6432.68	2.89	-3.69	36.8	7.82	30.5	7.95	38.6	7.86	29.9	7.88	35.2	7.82
	6456.39	3.90	-2.19	62.4	7.94	51.2	8.03	58.7	7.86	50.6	7.97	54.5	7.82	57.8	8.02

Table 3—Continued

	λ	χ		H II 746		H II 916		H II 1593		H II 2126		H II 2284		H II 2311	
Ion	(Å)	(eV)	$\log gf$	EW	$\log N$	EW	$\log N$	EW	$\log N$	EW	$\log N$	EW	$\log N$	EW	$\log N$

Table 4. Equivalent Widths and Abundances

Ion	λ	χ	$\log gf$	H II 2366		H II 2406		H II 2462		H II 2880		H II 3179	
	(Å)	(eV)		EW	$\log N$	EW	$\log N$	EW	$\log N$	EW	$\log N$	EW	$\log N$
Fe I	5793.92	4.22	-1.70	47.8	7.65	43.1	7.61	48.0	7.64	43.5	7.54	26.3	7.58
	5856.10	4.29	-1.64	46.8	7.63	38.9	7.52	46.6	7.62	46.8	7.61	24.8	7.55
	5927.80	4.65	-1.09	57.3	7.61	50.5	7.54	58.3	7.61	55.2	7.55	34.2	7.52
	6089.57	5.02	-0.94	51.4	7.69	40.2	7.53	49.5	7.65	48.6	7.63	30.4	7.60
	6093.65	4.61	-1.50	47.2	7.80	32.6	7.55	41.2	7.68	43.5	7.72	24.1	7.66
	6096.67	3.98	-1.93	49.8	7.67	45.5	7.64	56.1	7.78	55.1	7.75	29.5	7.65
	6151.62	2.18	-3.29	72.5	7.66	55.4	7.38	70.5	7.59	73.2	7.61	36.8	7.51
	6165.36	4.14	-1.47	57.3	7.51	51.3	7.45	56.5	7.48	55.9	7.46	37.3	7.50
	6270.23	2.86	-2.71	71.3	7.74	61.2	7.61	72.9	7.74	65.9	7.59	44.8	7.70
	6627.56	4.55	-1.68	34.8	7.66	36.0	7.73	39.6	7.75	30.2	7.55	21.5	7.70
	6806.86	2.73	-3.21	56.8	7.76	43.5	7.56	56.3	7.73	57.1	7.73	23.7	7.62
	6839.84	2.56	-3.45	51.6	7.71	42.5	7.60	47.9	7.60	49.3	7.62
	6842.69	4.64	-1.32	48.5	7.65	44.5	7.62	49.5	7.67	52.8	7.72	32.5	7.67
	6857.25	4.07	-2.15	38.2	7.71	33.3	7.59	35.5	7.63	17.2	7.60
	6861.94	2.42	-3.89	41.1	7.76	36.9	7.64	36.6	7.61	11.0	7.60
	6862.50	4.56	-1.57	44.5	7.74	38.4	7.62	25.3	7.68
	7284.84	4.14	-1.75	57.5	7.73
	7461.53	2.56	-3.58	42.4	7.59	34.2	7.51	44.8	7.62	42.0	7.54	18.9	7.67
	7547.90	5.10	-1.35	24.3	7.64	30.1	7.74
Fe II	5264.81	3.23	-3.13	34.0	7.69	37.8	7.61	36.9	7.84	38.9	7.95	51.4	7.48
	5414.05	3.22	-3.65	23.5	7.86	21.6	7.86	30.3	7.53
	5425.25	3.20	-3.39	33.8	7.91	36.1	7.79	30.8	7.88	34.8	8.07	48.1	7.63
	6084.10	3.20	-3.88	39.4	7.97	26.5	7.64
	6247.56	3.89	-2.44	41.0	7.86	51.3	7.90	38.0	7.86	34.5	8.05	66.6	7.64
	6432.68	2.89	-3.69	42.4	7.93	31.5	7.90	52.0	8.03	48.9	7.61
	6456.39	3.90	-2.19	51.2	7.87	60.8	7.86	50.8	7.93	74.1	7.53

Table 4—Continued

	λ	χ		H II 2366		H II 2406		H II 2462		H II 2880		H II 3179	
Ion	(Å)	(eV)	$\log gf$	EW	$\log N$	EW	$\log N$	EW	$\log N$	EW	$\log N$	EW	$\log N$

Table 5. Mean Iron Abundances

Star	[Fe I/H]	σ_μ^a	[Fe II/H]	σ_μ	ΔFe^b
H II 193	0.06	0.02	0.43	0.01	+0.37
H II 250	0.01	0.02	0.22	0.05	+0.21
H II 263	0.07	0.02	0.89	0.04	+0.82
H II 298	0.09	0.01	0.92	0.02	+0.83
H II 571	0.02	0.02	0.44	0.04	+0.42
H II 746	0.04	0.02	0.35	0.06	+0.31
H II 916	0.06	0.01	0.49	0.05	+0.43
H II 1593	0.00	0.01	0.35	0.02	+0.35
H II 2126	0.08	0.03	0.42	0.04	+0.34
H II 2284	0.05	0.03	0.28	0.06	+0.23
H II 2311	0.08	0.01	0.45	0.04	+0.37
H II 2366	0.09	0.02	0.34	0.04	+0.25
H II 2406	-0.02	0.01	0.33	0.05	+0.35
H II 2462	0.08	0.02	0.37	0.04	+0.29
H II 2880	0.04	0.02	0.53	0.02	+0.49
H II 3179	0.03	0.01	0.06	0.03	+0.03

^a $\sigma_\mu = \sigma_{s.d.}/\sqrt{N-1}$, where N is the number of lines measured.

^b $\Delta \text{Fe} = [\text{Fe II/H}] - [\text{Fe I/H}]$.

Table 6. Abundance Sensitivities

Star	Parameter	Fe I	Fe II
H II 263 ($T_{\text{eff}} = 5048$ K)	$\Delta T_{\text{eff}}(\pm 150$ K)	± 0.03	∓ 0.16
	$\Delta \log g(\pm 0.30$ dex)	± 0.01	$^{+0.11}_{-0.14}$
	$\Delta \xi(\pm 0.25$ km s $^{-1}$)	∓ 0.02	$^{-0.03}_{+0.01}$
H II 2284($T_{\text{eff}} = 5363$ K)	$\Delta T_{\text{eff}} = \pm 150$ K	$^{+0.07}_{-0.05}$	∓ 0.11
	$\Delta \log g = \pm 0.30$ dex	± 0.00	± 0.14
	$\Delta \xi = \pm 0.25$ km s $^{-1}$	∓ 0.03	$^{-0.05}_{+0.03}$
H II 3179($T_{\text{eff}} = 6172$ K)	$\Delta T_{\text{eff}} = \pm 150$ K	± 0.10	∓ 0.03
	$\Delta \log g = \pm 0.30$ dex	∓ 0.01	± 0.12
	$\Delta \xi = \pm 0.25$ km s $^{-1}$	∓ 0.02	∓ 0.06

Table 7. Census of Pleiades Cluster Metallicities

[Fe/H]	σ_{μ}	Reference
+0.13 ^a	0.06	Cayrel et al. (1988)
−0.03	0.02	Boesgaard et al. (1988)
+0.02	0.03	Boesgaard (1989)
−0.02	0.02	Boesgaard & Friel (1990)
+0.06 ^a	0.03	King et al. (2000a)
+0.06	0.01	Gebran & Monier (2008)
+0.03	0.05	Funayama et al. (2009)
+0.01	0.02	This work
+0.01	0.01	Mean

^aNot included in the Mean abundance, as described in the text.